Songklanakarin J. Sci. Technol.
45 (6), 627–637, Nov. – Dec. 2023

http://www.sjst.psu.ac.th

Original Article

Wave solution behaviors for fractional nonlinear fluid dynamic equation and shallow water equation

Weerachai Thadee[1], Jirapat Phookwanthong[1], Adisak Jitphusa[1], and Sirasrete Phoosree[2*]

[1] *Department of General Education, Faculty of Liberal Arts, Rajamangala University of Technology Srivijaya, Mueang, Songkhla, 90000 Thailand*

[2] *Education Program in Mathematics, Faculty of Education, Suratthani Rajabhat University, Mueang, Suratthani, 84100 Thailand*

Received: 10 June 2023; Revised: 14 October 2023; Accepted: 30 October 2023

Abstract

The behaviors of wave solutions of the fractional nonlinear space-time Sharma-Tasso-Olever equation and the fractional nonlinear space-time Estevez-Mansfield-Clarkson equation, representing a fluid dynamics equation and a shallow water equation, respectively, can be obtained by transforming the fractional nonlinear space-time partial differential equations into nonlinear ordinary differential equations with the Jumarie's Riemann-Liouville fractional derivative, and solving for a finite series form of solution in the Riccati sub-equation method. The newly discovered traveling wave solutions took the forms of generalized triangular functions and generalized hyperbolic functions, which ultimately led to the assessing physical wave behaviors. These behaviors are manifested in kink and periodic waves, and they are separately depicted by 2-D, 3-D and contour graphs. In addition, the results we received were more diverse than previous solutions.

Keywords: fractional Sharma-Tasso-Olever equation, fractional Estevez-Mansfield-Clarkson equation, Riccati sub-equation method, traveling wave solution

1. Introduction

In the fields of applied mathematics, applied science and engineering, the nonlinear evolution equations are very important equations that are employed in real-world scenarios. There are many models that have received attention in the context of fluid dynamics, fluid mechanics, neurons, optical fibers, electric circuits, water waves, plasma waves, capillary-gravity waves, plasma physics, chemical kinematics, chemical physics, etc. It is necessary to examine the techniques for solving the fractional nonlinear partial differential equations (PDEs) to conduct additional research into the behaviors of the aforementioned components. The investigation of solutions to fractional nonlinear PDEs is of academic interest because of the enhanced level of detail and generality exhibited by these solutions in comparison to conventional ones. Furthermore, it is feasible to make a comparison between graphs representing the physical solutions of different fractional orders. Mathematicians have developed and applied innovative and strong new methods in order to search for new outcomes of the exact traveling wave solutions, such as Khater II method (Khater, 2023; Zhao, Lu, Salama, Yongphet, & Khater, 2022), generalized Khater method (Khater, 2023), modified Khater method (Khater, 2023), G'/G-expansion method (Phoosree, & Chinviriyasit, 2021), G'/G^2-expansion method (Behera, Aljahdaly, & Virdi, 2022; Behera, & Aljahdaly, 2023), simple equation method (Phoosree, & Thadee, 2022; Sanjun, & Chankaew, 2022), Riccati-Bernoulli Sub-ODE (Alharbi, & Almatraf, 2020), Poincaré-Lighthill-Kuo method (Bhatti, & Lu, 2019), generalized Kudryashov method (Gaber, Aljohani, Ebaid, & Machado, 2019; Rahman, Habib, Ali, & Miah, 2019), modified Kudryashov method (Hao, Zhang, & Pang, 2019), fractional sub-equation method (Yépez-Martínez, & Gómez-Aguilar, 2019), Sardar sub-equation method (Khater, 2023;

*Corresponding author
Email address: sirasrete.pho@sru.ac.th

Khodadad, Nazari, Eslami, & Rezazadeh, 2017; Rehman, Iqbal, Subhi Aiadi, Mlaiki, & Saleem, 2022) and so on.

The Sharma-Tasso-Olever (STO) equation (Sheikh, Taher, Hossain, Akter, & Roshid, 2023) is a third order nonlinear evolution equation which has been used to explain a broad variety of physical processes, including the progression of nonlinear waves in fluid dynamics. The nonlinear STO equation has state $u = u(x, t)$ and $\hbar$ is a non-zero constant as shown here,

$$u_t + 3\hbar\left(u_x\right)^2 + 3\hbar u^2 u_x + 3\hbar u u_{xx} + \hbar u_{xxx} = 0. \tag{1}$$

Jianming, Jie and Wenjun (2011) have found 7 solutions to the STO equation by use of Bäcklund transformations. The found solutions are in the form of rational functions, exponential functions and hyperbolic functions.

The Estevez-Mansfield-Clarkson (EMC) equation (Mansfield, & Clarkson, 1997) is a nonlinear evolution equation of the fourth order that was developed from Mansfield and Clarkson's dispersion of patterns in liquid drop in 1997. This equation was used to study the behavior of waves in shallow water, and it is as follows:

$$u_{yyyt} + \varphi u_y u_{yt} + \varphi u_{yy} u_t + u_{tt} = 0, \tag{2}$$

where $u = u(x, y, t)$ and φ is a non-zero constant. The solution to nonlinear fractional space-and-time EMC equation by Kudryashov method (Thadee, Chankaew, & Phoosree, 2022) has one result in the form of an exponential functions, and the behaviors are found to be kink and periodic waves.

Definition 1. The fractional of Jumarie's Riemann-Liouville derivative (Jumarie, 2006) is given with the fractional derivative of order Φ as follows,

$$D_t^{\Phi} f(t) = f(t), \quad \Phi = 0, \tag{3}$$

$$D_t^{\Phi} f(t) = \frac{1}{\Gamma(1-\Phi)} \frac{d}{dt} \int_0^t (t-\beta)^{-\Phi} \left[f(\beta) - f(0) \right] d\beta, \quad 0 < \Phi < 1, \tag{4}$$

$$D_t^{\Phi} f(t) = \frac{d^n}{dt^n} D_t^{\Phi-n} f(t), \; n \le \Phi < n+1 \text{ and } n \ge 1. \tag{5}$$

In the year 2009, Jumarie discovered the following fundamental properties of the fractional of Jumarie's Riemann-Liouville derivative (Jumarie, 2009):

$$D_t^{\Phi} t^m = \frac{\Gamma(m+1)}{\Gamma(m-\Phi+1)} t^{m-\Phi}, \quad m \ge 0, \tag{6}$$

$$D_t^{\Phi} \left[f(t) h(t) \right] = f(t) D_t^{\Phi} h(t) + h(t) D_t^{\Phi} f(t), \tag{7}$$

$$D_t^{\Phi} f\left[h(t)\right] = D_t^{\Phi} f\left[h(t)\right]\left[h'(t)\right]^{\Phi} = f_h'\left[h(t)\right] D_t^{\Phi} h(t). \tag{8}$$

As a result of our study, we have discovered many new exact traveling wave solutions of the fractional nonlinear space-time STO equation and the fractional nonlinear space-time EMC equation by combining the fractional Jumarie's Riemann-Liouville derivative and the algorithm of the Riccati sub-equation method. Some examples of wave behavior graphs in contour, 2-dimensional, and 3-dimensional plots are shown. Furthermore, the outcomes obtained exhibited wider variations compared to results from prior methodologies.

2. Algorithm of Riccati Sub-Equation Method

This section describes the Riccati sub-equation method for locating traveling wave solutions for conformable fractional partial differential equations. Consider the following nonlinear conformable fractional partial differential equation in three independent variables x, y and t:

$$M\left(u, D_t^{\Phi}u, D_x^{\Phi}u, D_y^{\Phi}u, D_t^{2\Phi}u, D_x^{2\Phi}u, D_y^{2\Phi}u, D_t^{\Phi}D_y^{\Phi}u, \ldots\right) = 0, \; t > 0, 0 < \Phi \le 1, \tag{9}$$

where $u = u(x, y, t)$ and M is a polynomial expression including those of the greatest order and those with nonlinear factors in u with its derivatives in fractional form.

The following five processes can be used in the Riccati sub equation method.

First: Transformation process

Establishing a solution and using wave transformation,

$$u(x, y, t) = U(\beta), \quad \beta = \frac{\alpha x^{\Phi}}{\Gamma(\Phi+1)} + \frac{\delta y^{\Phi}}{\Gamma(\Phi+1)} - \frac{\eta t^{\Phi}}{\Gamma(\Phi+1)}, \tag{10}$$

where β is a general term for the transformation of traveling waves, α, δ and η are non-zero constants with positive direction of traveling wave when $\eta > 0$ and negative direction when $\eta < 0$ (Phoosree, 2019). We substitute Equation (10) into Equation (9) to get

$$N\left(U,\frac{dU}{d\beta},\frac{d^2U}{d\beta^2},\frac{d^3U}{d\beta^3},\dots\right)=0, \tag{11}$$

where N is a polynomial including those of the greatest order and those with nonlinear factors in U with its derivatives.
Second: Solution assuming process
Assume the solution to Equation (11) is in the form of a finite series,

$$U(\beta)=\sum_{i=0}^{P}c_iW^i(\beta), \tag{12}$$

when C_i are constants with C_P is non-zero.
Third: General solutions of Riccati sub equation method
The Riccati sub equation method (Khodadad, Nazari, Eslami, & Rezazadeh, 2017) is used to find W as shown below:

$$W'(\beta)=\rho+W^2(\beta), \tag{13}$$

where ρ is an arbitrary constant. The general solutions of Equation (13) are expressed in three cases as follows.
Case I: when $\rho < 0$,

$$W_1(\beta)=-\sqrt{-\rho}\tanh_{pq}\left(\sqrt{-\rho}\beta\right), \tag{14}$$

$$W_2(\beta)=-\sqrt{-\rho}\coth_{pq}\left(\sqrt{-\rho}\beta\right), \tag{15}$$

$$W_3(\beta)=-\sqrt{-\rho}\tanh_{pq}\left(2\sqrt{-\rho}\beta\right)\pm i\sqrt{-\rho}\,\mathrm{sech}_{pq}\left(2\sqrt{-\rho}\beta\right), \tag{16}$$

$$W_4(\beta)=-\sqrt{-\rho}\coth_{pq}\left(2\sqrt{-\rho}\beta\right)\pm \sqrt{-\rho}\,\mathrm{csch}_{pq}\left(2\sqrt{-\rho}\beta\right), \tag{17}$$

$$W_5(\beta)=-\frac{1}{2}\left(\sqrt{-\rho}\tanh_{pq}\left(\frac{\sqrt{-\rho}}{2}\beta\right)+\sqrt{-\rho}\coth_{pq}\left(\frac{\sqrt{-\rho}}{2}\beta\right)\right), \tag{18}$$

$$W_6(\beta)=\frac{\sqrt{-\left(Q^2+R^2\right)\rho}-Q\sqrt{-\rho}\cosh_{pq}\left(2\sqrt{-\rho}\beta\right)}{Q\sinh_{pq}\left(2\sqrt{-\rho}\beta\right)+R}, \tag{19}$$

$$W_7(\beta)=-\frac{\sqrt{-\left(R^2-Q^2\right)\rho}-Q\sqrt{-\rho}\sinh_{pq}\left(2\sqrt{-\rho}\beta\right)}{Q\cosh_{pq}\left(2\sqrt{-\rho}\beta\right)+R}, \tag{20}$$

where Q, R are nonzero constants with $R^2 - Q^2 > 0$.
Case II: when $\rho > 0$,

$$W_8(\beta)=\sqrt{\rho}\tan_{pq}\left(\sqrt{\rho}\beta\right), \tag{21}$$

$$W_9(\beta)=-\sqrt{\rho}\cot_{pq}\left(\sqrt{\rho}\beta\right), \tag{22}$$

$$W_{10}(\beta)=-\sqrt{\rho}\tan_{pq}\left(2\sqrt{\rho}\beta\right)\pm\sqrt{\rho}\sec_{pq}\left(2\sqrt{\rho}\beta\right), \tag{23}$$

$$W_{11}(\beta)=-\sqrt{\rho}\cot_{pq}\left(2\sqrt{\rho}\beta\right)\pm\sqrt{\rho}\csc_{pq}\left(2\sqrt{\rho}\beta\right), \tag{24}$$

$$W_{12}(\beta)=\frac{1}{2}\left(\sqrt{\rho}\tan_{pq}\left(\frac{\sqrt{\rho}}{2}\beta\right)-\sqrt{\rho}\cot_{pq}\left(\frac{\sqrt{\rho}}{2}\beta\right)\right), \tag{25}$$

$$W_{13}(\beta)=\frac{\pm\sqrt{\left(Q^2-R^2\right)\rho}-Q\sqrt{\rho}\cos_{pq}\left(2\sqrt{\rho}\beta\right)}{Q\sin_{pq}\left(2\sqrt{\rho}\beta\right)+R}, \tag{26}$$

$$W_{14}(\beta)=-\frac{\pm\sqrt{\left(Q^2-R^2\right)\rho}-Q\sqrt{\rho}\sin_{pq}\left(2\sqrt{\rho}\beta\right)}{Q\cos_{pq}\left(2\sqrt{\rho}\beta\right)+R}, \tag{27}$$

where Q, R are nonzero constants with $Q^2 - R^2 > 0$.

Case III: when $\rho = 0$,

$$W_{15}(\beta) = -\frac{1}{\beta + b}, \tag{28}$$

where b is a constant.

The different types of generalized triangular functions (Khodadad, Nazari, Eslami, & Rezazadeh, 2017) are defined as follows, with p and q arbitrary constants, $p > 0$, $q > 0$,

$$\sin_{pq}(\theta) = \frac{pe^{i\theta} - qe^{-i\theta}}{2i}, \tag{29}$$

$$\cos_{pq}(\theta) = \frac{pe^{i\theta} + qe^{-i\theta}}{2}, \tag{30}$$

$$\tan_{pq}(\theta) = -i\frac{pe^{i\theta} - qe^{-i\theta}}{pe^{i\theta} + qe^{-i\theta}}, \tag{31}$$

$$\cot_{pq}(\theta) = i\frac{pe^{i\theta} + qe^{-i\theta}}{pe^{i\theta} - qe^{-i\theta}}, \tag{32}$$

$$\sec_{pq}(\theta) = \frac{2}{pe^{i\theta} + qe^{-i\theta}}, \tag{33}$$

$$\csc_{pq}(\theta) = \frac{2i}{pe^{i\theta} - qe^{-i\theta}}, \tag{34}$$

where θ is an independent variable.

The different types of generalized hyperbolic functions (Khodadad, Nazari, Eslami, & Rezazadeh, 2017) are defined as follows, with p and q arbitrary constants, $p > 0$, $q > 0$,

$$\sinh_{pq}(\theta) = \frac{pe^{\theta} - qe^{-\theta}}{2}, \tag{35}$$

$$\cosh_{pq}(\theta) = \frac{pe^{\theta} + qe^{-\theta}}{2}, \tag{36}$$

$$\tanh_{pq}(\theta) = \frac{pe^{\theta} - qe^{-\theta}}{pe^{\theta} + qe^{-\theta}}, \tag{37}$$

$$\coth_{pq}(\theta) = \frac{pe^{\theta} + qe^{-\theta}}{pe^{\theta} - qe^{-\theta}}, \tag{38}$$

$$\mathrm{sech}_{pq}(\theta) = \frac{2}{pe^{\theta} + qe^{-\theta}}, \tag{39}$$

$$\mathrm{csch}_{pq}(\theta) = \frac{2}{pe^{\theta} - qe^{-\theta}}, \tag{40}$$

where θ is an independent variable.

Fourth: P exploring process

To obtain the positive integer P, equation (11) must be balanced for its highest order derivative term and its nonlinear term.

Fifth: Solutions reaching process

It is necessary to construct the parameters C_i, ($i = 1, 2, 3, \ldots, P$) and η by gathering the coefficients of all terms that have the same order W^i and then to set those coefficients to zero. When all the parameters in Equation (12) are substituted, the solutions to Equation (9) for the traveling wave are reached.

3. Application

The fractional nonlinear space-time STO equation and the fractional nonlinear space-time EMC equation have their traveling wave behaviors investigated here.

3.1 The fractional nonlinear space-time STO equation

The STO equation is a third-order nonlinear evolution equation that has been widely employed in the study of various physical phenomena, such as the propagation of nonlinear waves in fluid dynamics. The following is an explanation of the fractional nonlinear space-time STO equation,

$$D_t^{\Phi}u + 3\hbar\left(D_x^{\Phi}u\right)^2 + 3\hbar u^2 D_x^{\Phi}u + 3\hbar u D_x^{2\Phi}u + \hbar D_x^{3\Phi}u = 0,\ \ t > 0, 0 < \Phi \le 1, \tag{41}$$

where $u = u(x, t)$ and $\hbar$ is a non-zero constant. Equation (41) was transformed by equation (10) into an ordinary differential equation (ODE) without taking y into consideration,

$$-\eta\frac{dU}{d\beta} + 3\hbar\alpha^2\left(\frac{dU}{d\beta}\right)^2 + 3\hbar\alpha U^2\frac{dU}{d\beta} + 3\hbar\alpha^2 U\frac{d^2U}{d\beta^2} + \alpha^3\hbar\frac{d^3U}{d\beta^3} = 0. \tag{42}$$

After integration, the constant in Equation (42) is set to 0,

$$-\eta U + 3\alpha^2\hbar U\frac{dU}{d\beta} + \alpha\hbar U^3 + \alpha^3\hbar\frac{d^2U}{d\beta^2} = 0. \tag{43}$$

Then we utilized the balance approach of the highest order derivative term and the nonlinear term, thus $P = 1$. The equation (12) turned this into

$$U(\beta) = c_0 + c_1 W(\beta) \tag{44}$$

Equation (44) was now used in place of equation (43). In the fifth process, we grouped all the terms that corresponded to the same power of $W(\beta)$, and set each coefficient equal to zero as shown below,

$$W^0(\beta) : -\eta c_0 + 3\alpha^2\hbar c_0 c_1\rho + \alpha\hbar c_0^3 = 0, \tag{45}$$

$$W^1(\beta) : -\eta c_1 + 3\alpha^2\hbar c_1^2\rho + 3\alpha\hbar c_0^2 c_1 + 2\alpha^3\hbar c_1\rho = 0, \tag{46}$$

$$W^2(\beta) : 3\alpha^2\hbar c_0 c_1 + 3\alpha\hbar c_0 c_1^2 = 0, \tag{47}$$

$$W^3(\beta) : 3\alpha^2\hbar c_1^2 + \alpha\hbar c_1^3 + 2\alpha^3\hbar c_1 = 0. \tag{48}$$

Solving these equations, we get

$$c_1 = -\alpha \text{ and } \eta = 4\alpha\hbar c_0^2. \tag{49}$$

The following are the exact traveling wave solutions to the fractional nonlinear space-time STO equation:

Type I : when $\rho < 0$,

case 1 : $$u_1(x,t) = c_0 + \alpha\sqrt{-\rho}\tanh_{pq}\left(\sqrt{-\rho}\beta\right), \tag{50}$$

case 2 : $$u_2(x,t) = c_0 + \alpha\sqrt{-\rho}\coth_{pq}\left(\sqrt{-\rho}\beta\right), \tag{51}$$

case 3 : $$u_3(x,t) = c_0 + \alpha\sqrt{-\rho}\tanh_{pq}\left(2\sqrt{-\rho}\beta\right) \mp \alpha i\sqrt{-\rho}\,\mathrm{sech}_{pq}\left(2\sqrt{-\rho}\beta\right), \tag{52}$$

case 4 : $$u_4(x,t) = c_0 + \alpha\sqrt{-\rho}\coth_{pq}\left(2\sqrt{-\rho}\beta\right) \mp \alpha\sqrt{-\rho}\,\mathrm{csch}_{pq}\left(2\sqrt{-\rho}\beta\right), \tag{53}$$

case 5 : $$u_5(x,t) = c_0 + \frac{\alpha}{2}\left(\sqrt{-\rho}\tanh_{pq}\left(\frac{\sqrt{-\rho}}{2}\beta\right) + \sqrt{-\rho}\coth_{pq}\left(\frac{\sqrt{-\rho}}{2}\beta\right)\right), \tag{54}$$

case 6 : $$u_6(x,t) = c_0 - \alpha\left(\frac{\sqrt{-\left(Q^2+R^2\right)\rho} - Q\sqrt{-\rho}\cosh_{pq}\left(2\sqrt{-\rho}\beta\right)}{Q\sinh_{pq}\left(2\sqrt{-\rho}\beta\right) + R}\right), \tag{55}$$

case 7 : $$u_7(x,t) = c_0 + \alpha\left(\frac{\sqrt{-\left(R^2-Q^2\right)\rho} - Q\sqrt{-\rho}\sinh_{pq}\left(2\sqrt{-\rho}\beta\right)}{Q\cosh_{pq}\left(2\sqrt{-\rho}\beta\right) + R}\right), \tag{56}$$

where Q, R are nonzero constants with $R^2 - Q^2 > 0$.

Type II : when $\rho > 0$,

case 8 : $$u_8(x,t) = c_0 - \alpha\sqrt{\rho}\tan_{pq}\left(\sqrt{\rho}\beta\right), \tag{57}$$

case 9 : $$u_9(x,t) = c_0 + \alpha\sqrt{\rho}\cot_{pq}\left(\sqrt{\rho}\beta\right), \tag{58}$$

case 10 : $$u_{10}(x,t) = c_0 + \alpha\sqrt{\rho}\tan_{pq}\left(2\sqrt{\rho}\beta\right) \mp \alpha\sqrt{\rho}\sec_{pq}\left(2\sqrt{\rho}\beta\right), \tag{59}$$

$$\text{case 11}: \quad u_{11}(x,t) = c_0 + \alpha\sqrt{\rho}\cot_{pq}\left(2\sqrt{\rho}\beta\right) \mp \alpha\sqrt{\rho}\csc_{pq}\left(2\sqrt{\rho}\beta\right), \tag{60}$$

$$\text{case 12}: \quad u_{12}(x,t) = c_0 - \frac{\alpha}{2}\left(\sqrt{\rho}\tan_{pq}\left(\frac{\sqrt{\rho}}{2}\beta\right) - \sqrt{\rho}\cot_{pq}\left(\frac{\sqrt{\rho}}{2}\beta\right)\right), \tag{61}$$

$$\text{case 13}: \quad u_{13}(x,t) = c_0 - \alpha\left(\frac{\pm\sqrt{\left(Q^2-R^2\right)\rho} - Q\sqrt{\rho}\cos_{pq}\left(2\sqrt{\rho}\beta\right)}{Q\sin_{pq}\left(2\sqrt{\rho}\beta\right)+R}\right), \tag{62}$$

$$\text{case 14}: \quad u_{14}(x,t) = c_0 + \alpha\left(\frac{\pm\sqrt{\left(Q^2-R^2\right)\rho} - Q\sqrt{\rho}\sin_{pq}\left(2\sqrt{\rho}\beta\right)}{Q\cos_{pq}\left(2\sqrt{\rho}\beta\right)+R}\right), \tag{63}$$

where Q, R are nonzero constants with $Q^2 - R^2 > 0$.
Type III : when $\rho > 0$,

$$\text{case 15}: \quad u_{15}(x,t) = c_0 + \frac{\alpha}{\beta + b}, \quad b \text{ is a constant,} \tag{64}$$

where $\beta = \dfrac{\alpha x^{\Phi}}{\Gamma(\Phi+1)} - \dfrac{4\alpha\hbar c_0^2 t^{\Phi}}{\Gamma(\Phi+1)}$.

To obtain the physical wave behavior graphs, we set the parameters as shown in Table 1.

Table 1. Parameters set for some traveling wave solutions of the fractional nonlinear space-time STO equation

Solution	Parameters
Equation (50)	$c_0 = 1, \hbar = 1, \alpha = 0.2, \rho = -1, p = 1, q = 1, \Phi = 0.5, 10 \le x \le 30, 10 \le t \le 30$
Equation (51)	$c_0 = 1, \hbar = 1, \alpha = 0.2, \rho = -1, p = 1, q = 1, \Phi = 0.5, 10 \le x \le 30, 10 \le t \le 30$
Equation (53)	$c_0 = 1, \hbar = -1, \alpha = 0.2, \rho = -1, p = 1, q = 1, \Phi = 0.5, 10 \le x \le 30, 10 \le t \le 30$
Equation (54)	$c_0 = 1, \hbar = 0.1, \alpha = 0.2, \rho = -1, p = 1, q = 1, \Phi = 0.5, 10 \le x \le 30, 10 \le t \le 30$
Equation (55)	$c_0 = 1, \hbar = -0.1, \alpha = 0.2, \rho = -1, p = 1, q = 1, \Phi = 0.5, Q = -1, R = 2, 10 \le x \le 30, 10 \le t \le 30$
Equation (56)	$c_0 = 1, \hbar = -1, \alpha = 0.2, \rho = -1, p = 1, q = 1, \Phi = 0.5, Q = -1, R = 2, 10 \le x \le 30, 10 \le t \le 30$
Equation (64)	$c_0 = 1, \hbar = 0.1, \alpha = 0.2, \rho = -0, \Phi = 0.5, b = 1, 10 \le x \le 30, 10 \le t \le 30$

The physical wave behaviors of the fractional nonlinear space-time STO equation are shown in Figures 1-7.

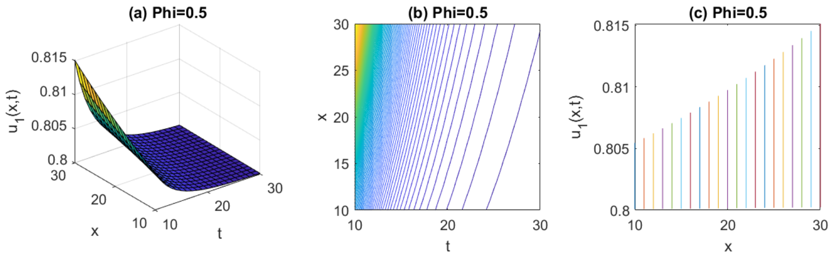

Figure 1. Kink graph in (a) 3-D, (b) contour, and (c) 2-D plot of equation (50)

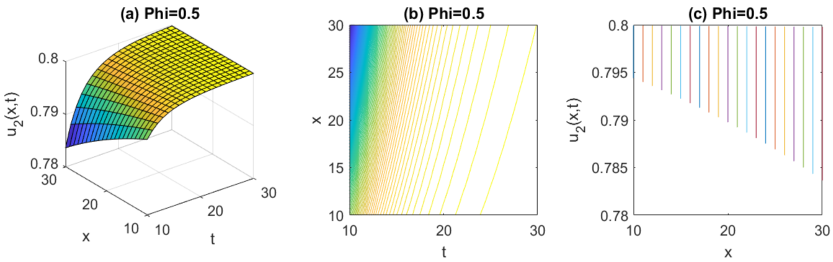

Figure 2. Kink graph in (a) 3-D, (b) contour, and (c) 2-D plot of equation (51)

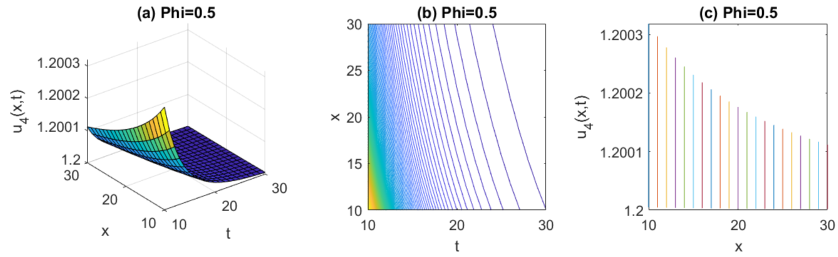

Figure 3. Kink graph in (a) 3-D, (b) contour, and (c) 2-D plot of equation (53)

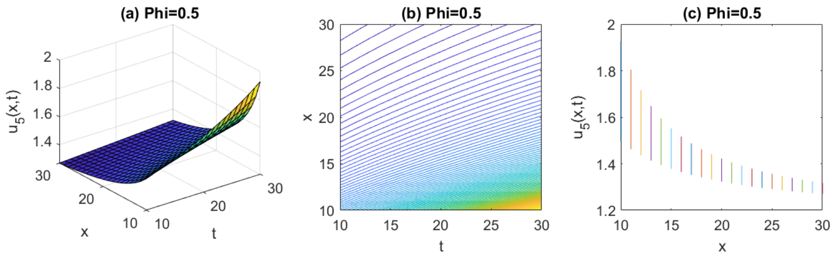

Figure 4. Kink graph in (a) 3-D, (b) contour, and (c) 2-D plot of equation (54)

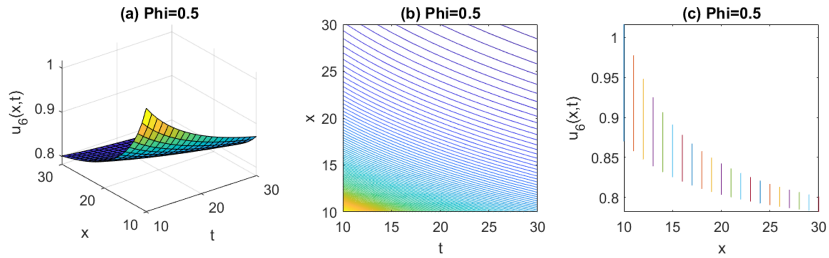

Figure 5. Kink graph in (a) 3-D, (b) contour, and (c) 2-D plot of equation (55)

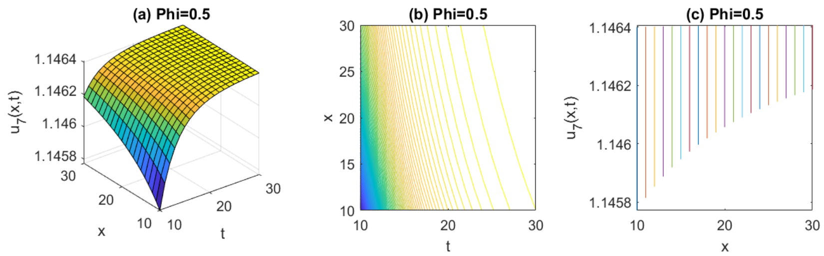

Figure 6. Kink graph in (a) 3-D, (b) contour, and (c) 2-D plot of equation (56)

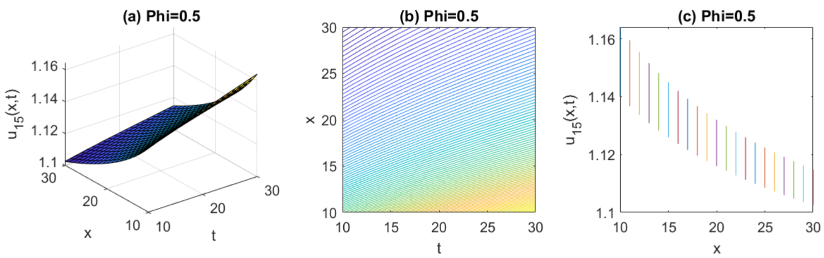

Figure 7. Kink graph in (a) 3-D, (b) contour, and (c) 2-D plot of equation (64)

3.2 The fractional nonlinear space-time EMC equation

The EMC equation is based on the study of dispersion pattern in liquid droplets. The equation under consideration was employed in the analysis of wave dynamics in shallow water. The fractional nonlinear space-time EMC equation (Thadee, Chankaew, & Phoosree, 2022) of the fourth order is as follows,

$$D_y^{3\Phi}D_t^{\Phi}u+\varphi D_y^{\Phi}uD_y^{\Phi}D_t^{\Phi}u+\varphi D_y^{2\Phi}uD_t^{\Phi}u+D_y^{2\Phi}u=0,\ t>0, 0<\Phi\le 1, \tag{65}$$

where $u = u(x, y, t)$ and φ is a non-zero constant. Applying the first process, the equation (65) becomes an ODE,

$$-\delta^3\frac{d^4U}{d\beta^4}-2\delta^2\varphi\frac{dU}{d\beta}\cdot\frac{d^2U}{d\beta^2}+\eta\frac{d^2U}{d\beta^2}=0. \tag{66}$$

Using once integration with zero constant,

$$-\delta^3\frac{d^3U}{d\beta^3}-2\delta^2\varphi\left(\frac{dU}{d\beta}\right)^2+\eta\frac{dU}{d\beta}=0. \tag{67}$$

After that, we used the P exploring process, giving $P = 1$. We get equation (44) again, substituting this equation to equation (67). In the fifth process, the system of equations is as follows,

$$W^0(\beta):\quad -2c_1\delta^3\rho^2-c_1^2\delta^2\varphi\rho^2+\eta c_1\rho=0, \tag{68}$$

$$W^2(\beta):\quad -8c_1\delta^3\rho-2c_1^2\delta^2\varphi\rho+\eta c_1=0, \tag{69}$$

$$W^4(\beta):\quad -6c_1\delta^3-c_1^2\delta^2\varphi=0. \tag{70}$$

The solution of the system of equations (68)-(70) is

$$c_1=-\frac{6\delta}{\varphi},\ \ \eta=-4\delta^3\rho. \tag{71}$$

The 15 cases of the exact traveling wave solutions of the fractional nonlinear space-time EMC equation are obtained below:
Type I : when $\rho < 0$,

case 1 : $$u_1(x,y,t)=c_0+\frac{6\delta}{\varphi}\left(\sqrt{-\rho}\tanh_{pq}\left(\sqrt{-\rho}\beta\right)\right), \tag{72}$$

case 2 : $$u_2(x,y,t)=c_0+\frac{6\delta}{\varphi}\left(\sqrt{-\rho}\coth_{pq}\left(\sqrt{-\rho}\beta\right)\right), \tag{73}$$

case 3 : $$u_3(x,y,t)=c_0-\frac{6\delta}{\varphi}\left(-\sqrt{-\rho}\tanh_{pq}\left(2\sqrt{-\rho}\beta\right)\pm i\sqrt{-\rho}\,\mathrm{sech}_{pq}\left(2\sqrt{-\rho}\beta\right)\right), \tag{74}$$

case 4 : $$u_4(x,y,t)=c_0-\frac{6\delta}{\varphi}\left(-\sqrt{-\rho}\coth_{pq}\left(2\sqrt{-\rho}\beta\right)\pm\sqrt{-\rho}\,\mathrm{csch}_{pq}\left(2\sqrt{-\rho}\beta\right)\right), \tag{75}$$

case 5 : $$u_5(x,y,t)=c_0-\frac{6\delta}{\varphi}\left(-\frac{1}{2}\left(\sqrt{-\rho}\tanh_{pq}\left(\frac{\sqrt{-\rho}}{2}\beta\right)+\sqrt{-\rho}\coth_{pq}\left(\frac{\sqrt{-\rho}}{2}\beta\right)\right)\right), \tag{76}$$

case 6 : $$u_6(x,y,t)=c_0-\frac{6\delta}{\varphi}\left(\frac{\sqrt{-\left(Q^2+R^2\right)\rho}-Q\sqrt{-\rho}\cosh_{pq}\left(2\sqrt{-\rho}\beta\right)}{Q\sinh_{pq}\left(2\sqrt{-\rho}\beta\right)+R}\right), \tag{77}$$

case 7 : $$u_7(x,y,t)=c_0-\frac{6\delta}{\varphi}\left(\frac{\sqrt{-\left(R^2-Q^2\right)\rho}-Q\sqrt{-\rho}\sinh_{pq}\left(2\sqrt{-\rho}\beta\right)}{Q\cosh_{pq}\left(2\sqrt{-\rho}\beta\right)+R}\right), \tag{78}$$

where Q, R are two nonzero real constants and satisfy $R^2 - Q^2 > 0$.
Type II: when $\rho < 0$,

case 8 : $$u_8(x,y,t)=c_0-\frac{6\delta}{\varphi}\left(\sqrt{\rho}\tan_{pq}\left(\sqrt{\rho}\beta\right)\right), \tag{79}$$

case 9 : $$u_9(x,y,t)=c_0+\frac{6\delta}{\varphi}\left(\sqrt{\rho}\cot_{pq}\left(\sqrt{\rho}\beta\right)\right), \tag{80}$$

$$\text{case } 10: \quad u_{10}(x,y,t)=c_0-\frac{6\delta}{\varphi}\left(-\sqrt{\rho}\tan_{pq}\left(2\sqrt{\rho}\beta\right)\pm\sqrt{\rho}\sec_{pq}\left(2\sqrt{\rho}\beta\right)\right), \tag{81}$$

$$\text{case } 11: \quad u_{11}(x,y,t)=c_0-\frac{6\delta}{\varphi}\left(-\sqrt{\rho}\cot_{pq}\left(2\sqrt{\rho}\beta\right)\pm\sqrt{\rho}\csc_{pq}\left(2\sqrt{\rho}\beta\right)\right), \tag{82}$$

$$\text{case } 12: \quad u_{12}(x,y,t)=c_0-\frac{6\delta}{\varphi}\left(\frac{1}{2}\left(\sqrt{\rho}\tan_{pq}\left(\frac{\sqrt{\rho}}{2}\beta\right)-\sqrt{\rho}\cot_{pq}\left(\frac{\sqrt{\rho}}{2}\beta\right)\right)\right), \tag{83}$$

$$\text{case } 13: \quad u_{13}(x,y,t)=c_0-\frac{6\delta}{\varphi}\left(\frac{\pm\sqrt{\left(Q^2-R^2\right)\rho}-Q\sqrt{\rho}\cos_{pq}\left(2\sqrt{\rho}\beta\right)}{Q\sin_{pq}\left(2\sqrt{\rho}\beta\right)+R}\right), \tag{84}$$

$$\text{case } 14: \quad u_{14}(x,y,t)=c_0+\frac{6\delta}{\varphi}\left(\frac{\pm\sqrt{\left(Q^2-R^2\right)\rho}-Q\sqrt{\rho}\sin_{pq}\left(2\sqrt{\rho}\beta\right)}{Q\cos_{pq}\left(2\sqrt{\rho}\beta\right)+R}\right), \tag{85}$$

where Q, R are two nonzero real constants and satisfy $Q^2 - R^2 > 0$.
Type III: when $\rho = 0$,

$$\text{case } 15: \quad u_{15}(x,y,t)=c_0+\frac{6\delta}{\varphi}\left(\frac{1}{\beta+b}\right), \quad b \text{ is a constant}, \tag{86}$$

where $\beta=\frac{\alpha x^{\Phi}}{\Gamma(\Phi+1)}+\frac{\delta y^{\Phi}}{\Gamma(\Phi+1)}+\frac{4\delta^3\rho t^{\Phi}}{\Gamma(\Phi+1)}.$

By adjusting the parameters in Table 2, we were able to generate the physical wave behavior graphs.

Figures 8-10 are graphical representations of the physical wave behavior of the solutions associated with the fractional nonlinear space-time EMC equation.

Table 2. Parameters set for some traveling wave solutions of the fractional nonlinear space-time EMC equation

Solution	Parameters
Equation (72)	$c_0=0,\varphi=1,\alpha=1,\delta=1,\rho=-1,\ p=1,q=1,\Phi=0.5, 0\le x\le 60,\ 0\le y\le 60, t=5,10$
Equation (73)	$c_0=0,\varphi=1,\alpha=1,\delta=1,\rho=-1,\ p=1,q=1,\Phi=0.5, 0\le x\le 60,\ 0\le y\le 60, t=5,10$
Equation (86)	$c_0=0,\varphi=1,\alpha=1,\delta=1,\rho=-1,\Phi=0.5, 0\le x\le 60, 0\le y\le 60, t=5,10$

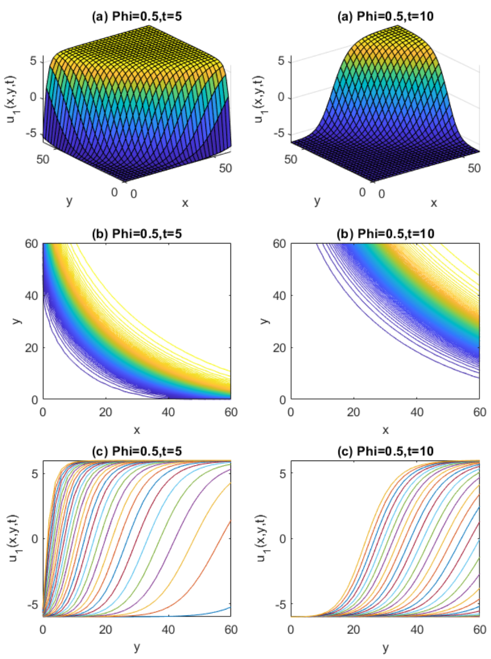

Figure 8. Kink graph in (a) 3-D, (b) contour, and (c) 2-D plot for t = 5, 10 in equation (72)

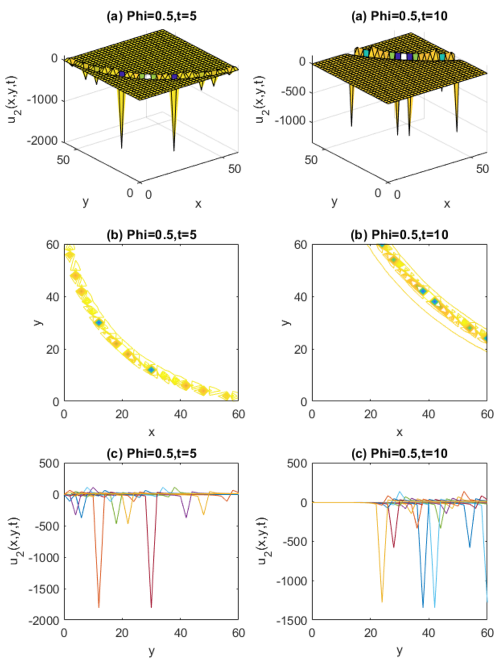

Figure 9. Periodic graph in (a) 3-D, (b) contour, and (c) 2-D plot for t = 5, 10 in equation (73)

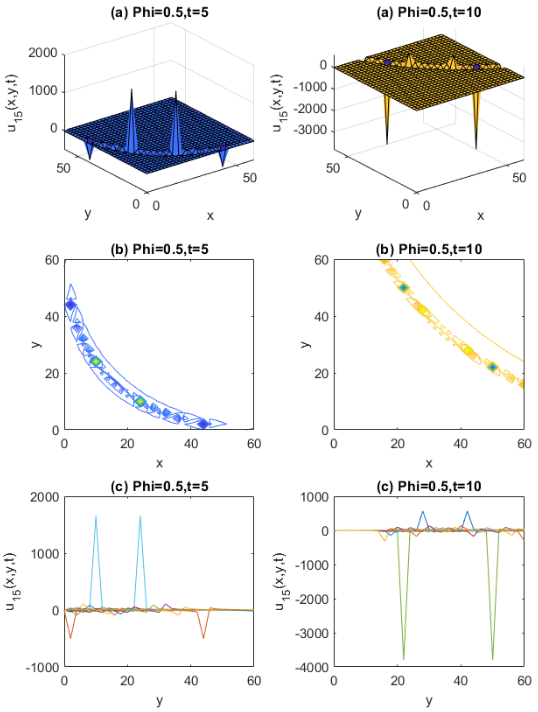

Figure 10. Periodic graph in (a) 3-D, (b) contour, and (c) 2-D plot for t = 5, 10 in equation (86)

5. Conclusions

The Riccati sub-equation method, in conjunction with the Jumarie's Riemann-Liouville fractional derivative showed 15 different traveling wave solutions of the fractional nonlinear space-time STO equation. We displayed several of the physical wave behavior graphs in 3-D, contour, and 2-D plots, after we set the parameters in Table 1. They all showed kink waves, traveling waves which increase or decrease from one state to another (Phoosree, 2019), as seen in Figures 1 – 7. These new solutions are more diverse than those of Jianming, Jie and Wenjun (2011), where they had seven solutions in the form of rational functions, exponential functions and hyperbolic functions. In the same approach as before, we set the parameters in Table 2 for the purpose of displaying some of the traveling wave solutions of the fractional nonlinear space-time EMC equation, as well as the physical wave behavior graphs that presented kink waves shown in Figure 8. The periodic waves, traveling wave solutions that are periodic (Phoosree, 2019), may be seen in Figures 9 and 10. The newly obtained precise solutions for this equation exhibit a greater degree of diversity in comparison to the previously obtained answers, where Thadee, Chankaew, & Phoosree (2022) found one solution in the form of an exponential function and behavior was found to be kink and periodic waves.

Acknowledgements

The authors would like to thank the reviewers for their insightful remarks and ideas, which facilitated the development of this paper.

References

Alharbi, A. R., Almatraf, M. B. (2020). Riccati-Bernoulli Sub-ODE approach on the partial differential equations and applications. *International Journal of Mathematics and Computer Science*, *15*(1), 367-388.

Behera, S., & Aljahdaly, N. H. (2023). Nonlinear evolution equations and their traveling wave solutions in fluid media by modified analytical method. *Pramana – Journal of Physics*, *97*, 130. doi:10.1007/s12043-023-02602-4

Behera, S., Aljahdaly, N. H., & Virdi, J. P. S. (2022). On the modified (G'/G^2)-expansion method for finding some analytical solutions of the traveling waves, *Journal of Ocean Engineering and Science*, *7*(4), 313-320. doi:10.1016/j.joes.2021.08.013

Bhatti, M. M., & Lu, D. Q. (2019). Analytical study of the head-on collision process between hydroelastic solitary waves in the presence of a uniform current. *Symmetry*, *11*(3), 333. doi:10.3390/sym11030333

Bhatti, M. M., & Lu, D. Q. (2019). An application of Nwogu's Boussinesq model to analyze the head-on collision process between hydroelastic solitary waves. *Open Physics*, *17*, 177-191. doi:10.1515/phys-2019-0018

Gaber, A. A., Aljohani, A. F., Ebaid, A., & Machado, J. T. (2019). The generalized Kudryashov method for nonlinear space-time fractional partial differential equations of Burgers type. *Nonlinear Dynamics*, *95*, 361-368. doi:10.1007/s11071-018-4568-4

Hao, M., Zhang, Y., & Pang, J. (2019). Solving fractional nonlinear partial differential equations by the modified Kudryashov method. *Journal of Physics: Conference Series*, *1300*, 012059. doi:10.1088/1742-6596/1300/1/012059

Jianming, L., Jie, D., & Wenjun, Y. (2011). Bäcklund Transformation and New Exact Solutions of the Sharma-Tasso-Olver Equation. *Abstract and Applied Analysis*, *2011*, 935710. doi:10.1155/2011/935710

Jumarie, G. (2006). Modified Riemann-Liouville derivative and fractional Taylor series of non-differentiable functions further results. *Computers and Mathematics with Applications*, *51*(9-10), 1367-1376. doi:10.1016/j.camwa.2006.02.001

Jumarie, G. (2009). Table of some basic fractional calculus formulae derived from a modified Riemann-Liouville derivative for non-differentiable functions. *Applied Mathematics Letters*, *22*(3), 378-385. doi:10.1016/j.aml.2008.06.003

Khater, M. M. (2023). Multi-vector with nonlocal and non-singular kernel ultrashort optical solitons pulses waves in birefringent fibers. *Chaos, Solitons and Fractals*, *167*, 113098. doi:10.1016/j.chaos.2022.113098

Khater, M. M. (2023). Novel computational simulation of the propagation of pulses in optical fibers regarding the dispersion effect. *International Journal of Modern Physics B*, *37*(09), 2350083. doi:10.1142/S0217979223500832

Khater, M. M. (2023). Prorogation of waves in shallow water through unidirectional Dullin–Gottwald–Holm model; computational simulations. *International Journal of Modern Physics B*, *37*(08), 2350071. doi:10.1142/S0217979223500716

Khodadad, F. S., Nazari, F., Eslami, M., & Rezazadeh, H. (2017). Soliton solutions of the conformable fractional Zakharov–Kuznetsov equation with dual-power law nonlinearity. *Optical and Quantum Electronics*, *49*, 384. doi:10.1007/s11082-017-1225-y

Mansfield, E. L., & Clarkson, P. A. (1997). Symmetries and exact solutions for a 2+1-dimensional shallow water wave equation. *Mathematics and Computer in Simulation*, *43*(1), 39-55. doi:10.1016/S0378-4754(96)00054-7

Phoosree, S. (2019). Exact solutions for the Estevez-Mansfield-Clarkson equation (Doctoral thesis, King Mongkut's University of Technology Thonburi, Bangkok, Thailand).

Phoosree, S., & Chinviriyasit, S. (2021). New analytic solutions of some fourth-order nonlinear space-time fractional partial differential equations by *G*' / *G*-expansion method. *Songklanakarin Journal of Science and Technology*, *43*(3), 795-801. doi:10.14456/sjst-psu.2021.105

Phoosree, S., & Thadee, W. (2022). Wave effects of the fractional shallow water equation and the fractional optical fiber equation. *Frontiers in Applied Mathematics and Statistics*, *8*, 900369. doi:10.3389/fams.2022.900369

Rehman, H. U., Iqbal, I., Subhi Aiadi, S., Mlaiki, N., & Saleem, M. S. (2022). Soliton solutions of Klein–Fock–Gordon equation using Sardar sub-equation method. *Mathematics*, *10*(18), 3377. doi:10.3390/math10183377

Rahman, M. M., Habib, M. A., Ali, H. M. S., & Miah, M. M. (2019). The generalized Kudryashov method: A renewed mechanism for performing exact solitary wave solutions of some NLEEs. *Journal of mechanics of continua and mathematical sciences*, *14*(1), 323-339. doi:10.26782/jmcms.2019.02.00022

Sanjun, J., & Chankaew, A. (2022). Wave solutions of the DMBBM equation and the cKG equation using the simple equation method. *Frontiers in Applied Mathematics and Statistics*, *8*, 952668. doi:10.3389/fams.2022.952668

Sheikh, M. A. N., Taher, M. A., Hossain, M. M., Akter, S., & Roshid, H. O. (2023). Variable coefficient exact solution of Sharma–Tasso–Olver model by enhanced modified simple equation method. *Partial Differential Equations in Applied Mathematics*, *7*, 100527. doi:10.1016/j.padiff.2023.100527

Thadee, W., Chankaew, A., & Phoosree, S. (2022). Effects of wave solutions on shallow-water equation, optical-fibre equation and electric-circuit equation. *Maejo International Journal of Science and Technology*, *16*(3), 262-274.

Yépez-Martínez, H., & Gómez-Aguilar, J. F. (2019). Fractional sub-equation method for Hirota–Satsuma-coupled KdV equation and coupled mKdV equation using the Atangana's conformable derivative. *Waves in Random and Complex Media*, *29*(4), 678-693. doi:10.1080/17455030.2018.1464233

Zhao, D., Lu, D., Salama. S. A., Yongphet, P., & Khater, M. M. (2022). Novel and accurate solitary wave solutions of the conformable fractional nonlinear Schrödinger equation. *Journal of Low Frequency Noise, Vibration and Active Control*, *41*(2), 488-499. doi:10.1177/14613484211068962